



HAL
open science

The Extreme Kuiper Belt Binary 2001 QW322

Jean-Marc C. Petit, J. Kavelaars, B. Gladman, J. Margot, P. Nicholson, R. Jones, J. Wm. Parker, M. Ashby, A. Bagatin, P. Benavidez, et al.

► **To cite this version:**

Jean-Marc C. Petit, J. Kavelaars, B. Gladman, J. Margot, P. Nicholson, et al.. The Extreme Kuiper Belt Binary 2001 QW322. *Science*, 2008, 322 (5900), pp.432-434. 10.1126/science.1163148. hal-02374710

HAL Id: hal-02374710

<https://hal.science/hal-02374710>

Submitted on 12 Nov 2020

HAL is a multi-disciplinary open access archive for the deposit and dissemination of scientific research documents, whether they are published or not. The documents may come from teaching and research institutions in France or abroad, or from public or private research centers.

L'archive ouverte pluridisciplinaire **HAL**, est destinée au dépôt et à la diffusion de documents scientifiques de niveau recherche, publiés ou non, émanant des établissements d'enseignement et de recherche français ou étrangers, des laboratoires publics ou privés.

The extreme Kuiper Belt binary 2001 QW₃₂₂.

J-M. Petit^{1,3*}, J.J. Kavelaars², B.J. Gladman³, J.L. Margot⁴,
P.D. Nicholson⁴, R.L. Jones⁵, J.Wm. Parker⁶, M.L.N. Ashby⁷,
A. Campo Bagatin⁸, P. Benavidez⁸, J. Coffey³,
P. Rousset¹, O. Mousis¹, P.A. Taylor⁴

¹Observatoire de Besançon, France

²Herzberg Institute of Astrophysics, Canada

³University of British Columbia, Canada

⁴Cornell University, USA

⁵University of Washington, USA

⁶Southwest Research Institute, Boulder, USA

⁷Harvard-Smithsonian Center for Astrophysics, USA

⁸University of Alicante, Spain

*To whom correspondence should be addressed; E-mail: petit@obs-besancon.fr.

The study of binary Kuiper Belt objects help probe the dynamic conditions present during planet formation in the Solar System. We report on the mutual-orbit determination of 2001 QW₃₂₂, a Kuiper Belt binary with a very large separation whose properties challenge binary-formation and evolution theories. Six years of tracking indicate that the binary's mutual orbit period is $\approx 25\text{--}30$ years, that the orbit pole is retrograde and inclined $50\text{--}62^\circ$ from the ecliptic plane, and, most surprisingly, that the mutual orbital eccentricity is < 0.4 . The semimajor axis of $105,000\text{--}135,000$ km is 10 times that of other near-equal mass binaries. Because this weakly bound binary is prone to orbital disruption by interlopers, its lifetime in its present state is likely less than

1 Gy.

A combination of survey strategies and adaptive optics technologies has led to a surge in the discovery rate of binary minor planets. Since 2001, newly-discovered binaries in the main asteroid and Kuiper belts have been announced at the rate of about seven per year (1,2). There are now more than 100 binaries known, nearly half of which are Kuiper Belt Objects (KBOs). Measurements of the frequency of binary objects and their sizes and orbital configurations constrain their formation and evolution mechanisms, theories of planetesimal accretion and disruption, and the collisional history of the Kuiper belt.

Discovering and studying the mutual orbits of binary systems is currently the only way to directly determine KBO masses. Assuming that the optical properties of the KBO binaries are representative of the whole KBO population, one can link mass to apparent magnitude and hence estimate the total mass of the Kuiper Belt without requiring assumptions on albedo and density. Recent HST observations (3) indicate that KBOs display a wide range of albedos (8-40%, assuming unit density), which complicate estimating the total mass of the Kuiper belt using a luminosity function. Combined with thermal infrared observations, phase-function photometry or star occultation observations, direct determination of KBO masses leads to the determination of their density and bulk composition.

Here we report the mutual-orbit determination of the large-separation Kuiper Belt binary, 2001 QW₃₂₂ (4). This KBO was discovered in data acquired 24 August, 2001 at the Canada-France-Hawaii Telescope by the Canada-France Ecliptic Plane Survey team. The two components had identical magnitudes of $m_R \simeq 24.0$ within the measurement uncertainties, implying essentially equal sizes. Only one other equal-component binary was known at the time, asteroid (90) Antiope, with a magnitude difference of ~ 0.1 mag (5). However 2001 QW₃₂₂ was obviously exceptional because the measured separation of $\sim 4''$ at its distance of 43 AU corresponds to a sky-projected physical separation of 125,000 km (about one third of the distance from Earth

to the Moon), far larger than any other small body binary.

The large separation implied a mutual-orbit period of at least several years. Six years of tracking using 4-to-8 m class telescopes (Fig. 1) resolved that 2001 QW₃₂₂, an object in the *main* classical Kuiper belt (6), has a low-eccentricity mutual orbit with a separation of 105,000-135,000 km, greater than any other known minor-planet binary (7). The separation is so large that this nearly equal-mass binary should be incredibly fragile to dynamical disruption, and its continued existence in the middle of the main Kuiper Belt puts strong constraints on the history of the belt (8).

Within the roughly 0.1-magnitude observational uncertainties at discovery, the two components had identical brightnesses, a finding confirmed in 2002 (9). Assuming identical albedos, object size is proportional to square root of flux, so it is unclear which component is the largest (and thus the primary). We therefore obtained higher-precision photometric observations from 8-m class telescopes (Very Large Telescope (VLT), Gemini-North and Gemini-South) between 2002 and 2007 including broadband colors in *R*-band, *I*-band, and *V*-band (Tables S1, S2 and S3). From these data, it appears that the relative magnitudes of the two components are essentially the same in all measured colors; the color similarity implies a surface similarity that strengthens the assumption of equal albedos. The plentiful *R*-band data give a mean relative magnitude $m_b - m_a = -0.03 \pm 0.02$. For what follows, we therefore take the two components to have the same physical size. Using the magnitude $r_{G0303} = 23.7$ for both components, measured at a geocentric distance of $\Delta=43.4$ AU, we derive a radius of $r=54$ km for an assumed *r*-band albedo $p=0.16$. The color of 2001 QW₃₂₂ is on the blue extreme of the color distribution of the cold classical Kuiper belt (10) or the Kuiper Belt core (11). At the 1σ confidence level, both components could have a light curve of amplitude ~ 0.4 magnitude, but no rotation period could be derived.

We measured (Table S4) Right-Ascension (RA) and Declination (DEC) of the center of

mass (assuming equal mass components) of the binary, along with position angle and separation between components (Fig. 1). Fits to the astrometric measurements up to and including 2006 were equally consistent with a large-eccentricity mutual orbit either pole aligned or anti-aligned with the line of sight, as well as a low-eccentricity orbit viewed nearly edge-on. Additional measurements were acquired in October 2006 (from Gemini-South), and fall 2007 (September from Gemini-South, October from (VLT, November from Multi Mirror Telescope (MMT) and VLT), which ruled out nearly all $e > 0.3$ solutions. This is surprising as it is difficult to imagine how to bind two small bodies that never come closer to each other than 85,000 km. The mutual orbit of 2001 QW₃₂₂ is retrograde, with a pole's ecliptic latitude between -50° and -62° , and is viewed somewhat edge-on (inclined at $55-70^\circ$ to the line of sight).

There remain three main groups of acceptable orbits: one group with $e \approx 0.2$, $a \approx 114,000$ km, $P \approx 27$ yr, $\rho \approx 0.94$ g cm⁻³, another group with nearly-circular orbits $e \lesssim 0.05$, $a \approx 128,000$ km, $P \approx 29$ yr, $\rho \approx 1.11$ g cm⁻³, and a smaller group with $e \lesssim 0.4$, $a \approx 105,000$ km, $P \approx 18$ yr, $\rho \approx 1.6$ g cm⁻³ (Fig. 2). We mildly prefer the non-circular orbits which have a goodness-of-fit 10% better than for the nearly-circular group. The stability region for binary orbits can be expressed in terms of the ratio a/R_H , where R_H is the Hill radius (7), with prograde orbits becoming unstable for a/R_H greater than 0.3-0.4 (12), while the limit of stability of retrograde orbits is 0.5-0.6. This may explain why the first such system was found to be retrograde. It also indicate that 2001 QW₃₂₂ is very fragile to disruption as mentioned by (8). For our acceptable orbits, a/R_H varies mostly between 0.27 and 0.32, with the first group of orbits centered at 0.29, and the second group centered at 0.31.

According to Kepler's third law, the total mass of the binary is $0.9-2.4 \times 10^{18}$ kg; most of the estimated values are between 1.1×10^{18} and 1.5×10^{18} kg. With the photometrically-derived nominal size of $r=54$ km for each component (assumed albedo of 0.16), the density of 2001 QW₃₂₂ (Fig. 2, bottom-left) is likely $0.8-1.2$ g cm⁻³. This is a little higher than compa-

rably sized outer Solar System bodies (Figure 5 of *13*; $0.6\text{-}0.8 \text{ g cm}^{-3}$). Our nominal albedo of 0.16 is about double that estimated from optical and thermal infrared photometry for similar-size KBOs (*14, 15*), but about a factor of 2 below that of (58534) Logos/Zoe ($p = 0.37 \pm 0.04$; 2), which is of comparable size. Estimated density from eqs. S2 and S3 is proportional to the assumed albedo to the power $3/2$. Halving our albedo would increase our radius estimates by $\sqrt{2}$ and decrease the estimated density by a factor of $2^{3/2} = 2.8$, below the range of published densities (*13*) for such small bodies.

The nominal densities shown in Fig. 2 are at the boundary between the density of a low-porosity pure-water ice body, and that of a mixture of water ice and silicate rocks (*13*). A thermal detection, mutual eclipse, or stellar occultation by the binary (all unlikely) would be needed to further constrain the size, albedo, density, and hence the bulk composition of 2001 QW₃₂₂.

Given the very large separation (Fig. 3), such a binary is difficult to create and maintain. Of all the proposed KBO binary formation scenarios (*16-19*), only the collision of two bodies close to a third one (*16*) can simply explain the primordial formation of such a system (7).

A study of the long-term stability of the large-separation KB binaries (8) concluded that the major destabilizing factor is unbinding due to direct collisions of impactors on the secondary. Applying their method to the newly determined orbital and physical parameters for 2001 QW₃₂₂ and our nominal albedo, we find that the lifetime of this binary is 0.3-1 Gy, 2-3 times shorter than the previous estimate. This implies one of two things. Either 2001 QW₃₂₂ was created with its current mutual-orbit early in the history of the Solar System, in which case it is one of the few survivors of a population at least 50-100 times larger. Or this is a transitory object, evolving, due to perturbation from interactions with smaller KBOs, from a population of more tightly bound binaries. Asserting this latter hypothesis would require better orbital statistics for moderately large KB binaries (separation of 1-2'').

For the likely mutual-orbit parameters, the average orbital speed is $\langle v \rangle \simeq 0.85 \text{ m/s}$ or a

mere 3 km/h, a slow human walking pace. An observer standing on one of the components (a very precarious situation, as the gravity is only 0.02 m/s^2 or almost 600 times smaller than on Earth) would see the other component subtend an angle of only 3 arcmin; this corresponds to a pinhead seen at arm length. The existence of the other component would not be in doubt however, since when viewed at full phase it would be as luminous as Saturn seen from Earth, and move perceptibly week to week.

References and Notes

1. W.J. Merline, S.J. Weidenschilling, D.D. Durda, J.L. Margot, P. Pravec and A.D. Storrs, in *Asteroids III*, W.F. Bottke Jr., A. Cellino, P. Paolicchi, R.P. Binzel Eds. (Univ. Arizona Press, Tucson, AZ, 2002), pp. 289-312.
2. K.S. Noll, W.M. Grundy, E.I. Chiang, J.L. Margot, and S.D. Kern, in *The Solar System beyond Neptune*, A. Barucci, H. Boehnhardt, D. Cruikshank, A. Morbidelli Eds. (Univ. Arizona Press, Tucson, AZ, 2008), pp. 345-363.
3. J.L. Margot, M.E. Brown, C.A. Trujillo, R. Sari, J.A. Stansberry, *Bull. Amer. Astron. Soc.*, **37**, 737 (2005).
4. J.J. Kavelaars, J.-M. Petit, G. Gladman, M. Holman, *IAU Circ.*, **7749**, 1 (2001).
5. W.J. Merline, L.M. Close, C. Dumas, J.C. Shelton, F. Menard, C.R. Chapman, D.C. Slater, *Bull. Amer. Astron. Soc.*, **32**, 1017 (2000).
6. B. Gladman, B.G. Marsden, C. Van Laerhoven, in *The Solar System beyond Neptune*, A. Barucci, H. Boehnhardt, D. Cruikshank, A. Morbidelli Eds. (Univ. Arizona Press, Tucson, AZ, 2008), pp. 43-57.
7. See Supporting Online Material text.

8. J-M. Petit, O. Mousis, *Icarus*, **168**, 409 (2004).
9. J. Burns, V. Carruba, B. Gladman, B.G. Marsden, *Minor Planet Electronic Circ.*, **L30** (2002).
10. O.R. Hainaut, A.C. Delsanti, *Astron. Astrophys.*, **389**, 641 (2002).
11. A.A.S. Gulbis, J.L. Elliot, J.F. Kane, *Icarus*, **183**, 168 (2006).
12. D. Nesvorny, J.L.A. Alvarellos, L. Dones, H.F. Levison, *Astron. J.*, **126**, 398 (2003).
13. W.M. Grundy, J.A. Stansberry, K.S. Noll, D.C. Stephens, D.E. Trilling, S.D. Kern, J.R. Spencer, D.P. Cruikshank, H.L. Levison, *Icarus*, **191**, 286 (2007).
14. J.A. Stansberry, W.M. Grundy, J.L. Margot, D.P. Cruikshank, J.P. Emery, G.H. Rieke, D.T. Trilling, *Astrophys. J.*, **643**, 556 (2006).
15. J.R. Spencer, J.A. Stansberry, W.M. Grundy, K.S. Noll, *Bull. Am. Astron. Soc.*, **38**, 546 (2006).
16. S.J. Weidenschilling, *Icarus*, **160**, 212 (2002).
17. P. Goldreich, Y. Lithwick, R. Sari, *Nature*, **420**, 643 (2002).
18. Y. Funato, J. Makino, P. Hut, E. Kokubo, D. Kinoshita, *Nature*, **427**, 518 (2004).
19. S.A. Astakhov, E.A. Lee, D. Farrelly, *MNRAS*, **360**, 401 (2005).
20. This work was partially supported by NASA/Planetary Astronomy Program grant NNG04GI29G. ACB also acknowledges support from Ministerio de Educacion y Ciencia (Spain), National project n. AYA2005-07808-C03-03. JLM was partially supported by grant NNX07AK68G from the NASA Planetary Astronomy program. This research used the facilities of the

Canadian Astronomy Data Centre operated by the National Research Council of Canada with the support of the Canadian Space Agency. The Canada-France-Hawaii Telescope (CFHT) is operated by the National Research Council of Canada, the Institut National des Sciences de l'Univers of the Centre National de la Recherche Scientifique of France, and the University of Hawaii. Observations at Palomar Observatory are carried out under a collaborative agreement between Cornell University and the California Institute of Technology. Observations made with ESO Telescopes at the La Silla or Paranal Observatories under programme IDs 069.C-0460, 071.C-0497, 072.C-0542, 074.C-0379, 075.C-0251 and 380.C-0791. The Gemini Observatory is operated by the Association of Universities for Research in Astronomy, Inc., under a cooperative agreement with the NSF on behalf of the Gemini partnership: the National Science Foundation (United States), the Science and Technology Facilities Council (United Kingdom), the National Research Council (Canada), CONICYT (Chile), the Australian Research Council (Australia), Ministério da Ciência e Tecnologia (Brazil) and SECYT (Argentina). Observations obtained at WIYN Observatory, a joint facility of the University of Wisconsin-Madison, Indiana University, Yale University, and the National Optical Astronomy Observatories. Observations obtained at the William Herschel Telescope, at Roque de los Muchachos Observatory (La Palma, Canary Islands, Spain), operated by the Instituto de Astrofísica de Canarias. Observations reported here were obtained at the MMT Observatory, a joint facility of the Smithsonian Institution and the University of Arizona.

Fig. 1. (Top): image of the Kuiper Belt binary 2001 QW₃₂₂ from VLT, on September 3rd, 2002. The separation between the two components at the time was 3.4". (Middle): image from Gemini-South on September 17th, 2007; the separation was 1.8". On both panels, the components are circled. On all panels, North is up and East is left. The "a" component is the most southern one. (Bottom): relative position of the two components of 2001 QW₃₂₂. The origin corresponds to the center of mass, assuming equal mass for both components. The southern "a" component has been moving westward, while the northern "b" component has been moving to the east.

Fig. 2. Range of plausible orbital parameters and densities for 2001 QW₃₂₂. These have been obtained by non-linear minimisation of a χ^2 statistics, starting from several thousand initial conditions, retaining only those solutions with a reduced χ^2 close enough to the overall best-fit, as explained in (7). The fitted parameters are the binary's orbital period P , its semimajor axis a , its eccentricity e , its pole orientation and its argument of pericenter. Eccentricity (A), density (B) and semimajor axis (C) are given as a function of the period, and the pole's ecliptic latitude versus pole's ecliptic longitude (D). The density was derived assuming a radius for each component of 54 km. (D) shows the precision with which the mutual-orbit pole is now known on the sky.

Fig. 3. Secondary-to-primary mass ratio versus average separation (in units of the primary's radius). Represented by the dashed box are the known binary asteroids, all on the left side of the plot (the largest separation barely exceeds 100). Also shown are the most-extreme outer-planet irregular satellites and several other binary KBOs. The mass ratio q is estimated from the published difference in magnitude between the components, assuming an equal albedo and density for both components. The error bar on the separation for 2001 QW₃₂₂ accounts only for the uncertainty in the estimated semimajor axis a , but does not account for the (unlikely) possibility that the radius could be off by up to a factor of two. Nevertheless, with equal mass component and a separation that is more than 2000 times the radius of each component, 2001 QW₃₂₂ clearly stands out in the top-right corner of this diagram as the widest-orbit, near-equal mass binary of the Solar System.

Supporting material

Discovery and tracking

2001 QW₃₂₂ was discovered on Aug. 24, 2001, while conducting a search for satellites of Uranus (*S1*). The measured separation was 125,000 km, and the two components had identical magnitudes of $m_R \simeq 24.0$. Making common (in 2001) assumptions of 4% albedos and densities $\sim 1 \text{ g cm}^{-3}$, radii of order 100 km were derived. Assuming the separation was equal to the semimajor axis, a period estimate of ≈ 12 years resulted (*S2*). A mistaken use of diameter instead of radius for the period calculation caused the initial period estimate to be a factor of $\sqrt{8}$ too low; it should have been ~ 11 years instead of four years for the 100-km radius case. This was the second similar-sized component binary known at the time. Since then, binaries with similar-sized component have been discovered in most dynamical classes: the near-Earth asteroid Hermes (*S3*), several small main-belt asteroids (e.g. *S4*), the Trojan Patroclus (*S5*), and several KBO binaries (*S6*).

We began a tracking program to determine both the heliocentric orbit of the system as well as the mutual orbit of the binary. By 2003 sufficient observations were acquired to establish the heliocentric orbit (see below) and yielded a relatively ‘normal’ trans-neptunian object in the so-called ‘main’ classical belt (*S7*), with semimajor axis $a_\odot=44$ AU, eccentricity $e=0.024$, inclination $i=4.8^\circ$, and a distance of $R=44$ AU from the Sun at time of discovery. However, in the two years after discovery the on-sky separation had only changed by about an arcsecond, implying an orbital period of at least a decade. At this point, and for several more years, it was unclear if the mutual orbit had a large eccentricity (with an orbital plane in the plane of the sky) or a nearly-circular orbit viewed close to edge-on.

Both possibilities remained open for the following years and estimates for the orbital period increased to well past a decade. By 2006 it became clear that the closest projected separation would occur in 2007, and we acquired a series of high-quality observations on 8-meter class telescopes. These observations have resulted in the virtual elimination of the high-eccentricity solutions, and we thus here report that 2001 QW₃₂₂ has a low-eccentricity orbit with a record-breaking separation for a small-body binary, having an orbital period measured in decades.

Photometric observations

Apparent magnitudes are related to physical size and albedo by Russell’s formula (*S8*):

$$m_X = M_{\odot,X} - 2.5 \log_{10} \left[p_X \left(\frac{r}{R} \right)^2 \frac{1}{\Delta_{AU}^2} \right] \quad (\text{S1})$$

where M_\odot is the Sun’s brightness at 1 AU in the appropriate filter X , R is the heliocentric distance (in the same units as the object radius r), and Δ_{AU} is the geocentric distance in AU. One thus relates the object’s apparent magnitude, its distance to the Sun and the Earth, its radius

r and its geometric albedo p . From this we derive the dimensionless ratio r/R expressing the body's size as a function of measured and/or assumed quantities:

$$\left(\frac{r}{R}\right) = 110 \times \frac{\Delta_{AU}}{44} \times 10^{\frac{M_{\odot,X}-m_X}{5}} \times \sqrt{\frac{0.16}{p_X}}. \quad (\text{S2})$$

Note that the estimated radius r depends principally on measured quantities (m_X , Δ_{AU} , R and $M_{\odot,X}$), and only weakly on the assumed value of the albedo p_X (inverse square root). In the above formula, we scale distances from the Earth to 44 AU since this is the typical distance to the main classical Kuiper Belt. We elected to use $p_X=0.16$ as our nominal scaling value since it is in the range of the most recent estimates, and a factor of four from the lower and upper extreme values for albedo of small bodies (hence the derived radius is within a factor of two of its real value). For the CFHT R filter and the AB system used in our initial observations, $M_{\odot}=-26.94$ (*S9-S11*). Our observations occurred at opposition, at a geocentric distance of $\Delta=43.3$ AU (and heliocentric distance of 44.3 AU). Hence each component of magnitude $m_R=24$ gives an estimate of $r=50$ km for the nominal albedo $p_R=0.16$.

Because our initial flux measurements showed that both components of 2001 QW₃₂₂ have essentially the same apparent magnitude (implying identical sizes under the assumption of similar albedo), we obtained photometric observations in the R -band, I -band and V -band filters from 8-m class telescopes (VLT and Gemini North and South telescopes) between 2002 and 2007. Tables S1, S2 and S3 give the relative magnitude of the two components (component “a” minus component “b”), together with the apparent magnitude of each component. Table S1 lists photometric measurements for R -band filters: the R_{BESS} filter on VLT/FORS1 in 2002, $R_{SPECIAL}$ filter on VLT/FORS2 for all other VLT images, r_{G0303} filter on Gemini-N in 2005 and r filter on Gemini-S in 2006 and 2007. Table S2 lists photometric measurements for V -band filters: the V_{BESS} filter on VLT/FORS2 in 2003 and 2007, and g_{G0301} filter on Gemini-N in 2005. Table S3 lists photometric measurements for I -band filters: the I_{BESS} filter on VLT/FORS2 in 2003 and 2007, and i_{G0302} filter on Gemini-N in 2005.

Column two of Table S1 implies a possible variation of the relative magnitudes of up to 0.6 magnitude at a 2.2σ confidence level. This level of confidence is derived from the uncertainties reported in the same column, which are those reported by the PHOT or ALLSTAR tasks in IRAF¹. However, a close look at the variation of the relative magnitude in Gemini-N i_{G0302} filter in 2005, all taken within 20 minutes, indicates that the uncertainty reported here (photon counts statistical fluctuations) is probably underestimated, making the previous variations more likely a result at the 1.5σ confidence level only. But we cannot quantify this more precisely. Similarly, the apparent magnitude data seem to imply a possible variability of the apparent magnitude of up to 0.45 magnitude for component “a”, and up to 0.35 magnitude for component “b”. For the fall 2007 VLT data, part of the variation could be due to phase effects. For the other VLT data spanning 1 to 4 days, the effect, if real, is more likely to be due to a rotation/shape related light

¹IRAF is distributed by the National Optical Astronomy Observatories, which are operated by the Association of Universities for Research in Astronomy (AURA), Inc., under cooperative agreement with the National Science Foundation.

curve. But again, this result is likely only at just above 1σ confidence level. A more definitive answer would require to get very accurate photometry (0.05 magnitude uncertainty or better) in at least 3 colors over two or more sequential nights. This can only be achieved using an 8-m class telescope or larger because the target is moving, preventing too long exposures.

Putting all the R-band relative magnitudes together, one derives a mean relative magnitude of $m_b - m_a = -0.03 \pm 0.02$ (Fig. S1). So for all intents and purposes, we will assume equal magnitudes for both components.

Comparing column 2 of Tables S1, S2 and S3, the relative magnitudes of the two components are essentially the same in all measured colors. Within the photon count statistical errors, the colors of the two components are identical. Several KBO binaries observed with HST appear to have similar colors (S12). This result supports the idea that both components have similar albedos. Since they also appear to have the same magnitude, they are most likely of the same physical size. Using the r_{G0303} filter data from Gemini North, we can make a better estimate of the size of 2001 QW₃₂₂ as a function of albedo. For this, we take for the magnitude of both components $r_{G0303} = 23.7$, measured at a geocentric distance of $\Delta=43.4$ AU. In this filter, the AB magnitude of the Sun is -26.93 (S9), yielding a size of $r=54$ km for the nominal albedo $p_R=0.16$.

Comparing our VLT data with the V-R versus R-I color-color plot in Fig. 2 from (S13), we see that 2001 QW₃₂₂ is on the blue extreme of the cold classical belt. This statement is also supported by our Gemini-N data, when compared to the Sloan g' , r' and i' colors of Kuiper belt Core objects given by (S14) in their Table 1 (Fig. S2).

The mutual orbit

Our orbit determination software uses the separation and position angle of the secondary with respect to the primary to solve for the orbital parameters in the two-body problem. The mutual orbital plane orientation is assumed constant, but heliocentric motions and light-time corrections are taken into account. Astrometric positions and their errors are specified at the mid-time of the exposure sequence. Starting from thousands of initial conditions, the software adjusts for seven parameters (six orbital elements plus the mass of the system) in the nonlinear ordinary least squares problem with a Levenberg-Marquardt technique. The covariance matrix and post-fit residuals are computed and inspected. Binary orbits have been computed with this algorithm for near-Earth asteroids (S15, S16), main-belt asteroids (S17, 18), Kuiper belt objects (S6), dwarf planets, and binary stars.

For 2001 QW₃₂₂, we used 92 measurements at 46 epochs, resulting in 85 degrees of freedom. The best-fit reduced χ^2 value was 0.526. Orbital fits with reduced χ^2 values exceeding the overall best-fit value by more than the statistically significant increase of 0.096 were eliminated. The valid solutions seem to cluster into three regions of the chi-square space, with the best-fit results near ($e \approx 0.2$, $a \approx 114,000$ km, $P \approx 27$ yr) and ($e \approx 0.4$, $a \approx 105,000$ km, $P \approx 18$ yr), and somewhat worse fits near ($e \lesssim 0.05$, $a \approx 128,000$ km, $P \approx 29$ yr). Thanks to the high

Signal-to-Noise ratio of most of our observations, and to the six years of arc, we are able to see the parallax of the object and resolve the degeneracy of which component is in the foreground and which is in the background. Hence we are able to resolve the initial degeneracy between prograde and retrograde orbits.

The Hill radius denotes the distance from a body at which the tidal forces due to the Sun and the gravitational force due to the body, both acting on a test particle, are in equilibrium. This roughly represent a region of stability for periodic orbits like the mutual orbit of binary objects. It is given by

$$R_H = a_\odot \left(\frac{M_b}{3M_\odot} \right) \quad (\text{S3})$$

where M_b is the total mass of the binary, a_\odot is its semi-major axis around the Sun and M_\odot the mass of the Sun. As mentioned above, the heliocentric semimajor axis is $a_\odot=44$ AU. Hence, the ratio a/R_H varies mostly between 0.27 and 0.32, with the first group of orbits centered at 0.29, and the second group centered at 0.31. It is interesting to note that the only other ‘‘binary’’ systems that have such a large value of the ratio a/R_H are irregular satellites of the giant planets.

From the dynamics of the mutual orbit, one can also derive an estimate of the size of the binary. Assuming both components have the same radius and density ρ , Newton’s form of Kepler’s third law gives the dimensionless ratio

$$\left(\frac{a}{r} \right)^3 = \frac{2G\rho}{3\pi} P^2 \quad (\text{S4})$$

where a is the binary’s mutual semimajor axis, G is the gravitational constant, and P is the period of the orbit. From the orbital fitting we obtain pairs of P and a , so taking $\rho \simeq 1 \text{ g cm}^{-3}$,

$$r \simeq 4.3 \times 10^{-3} \frac{a}{P^{2/3}} \quad (\text{S5})$$

where P is given in years and a in the same units as r . The $e \approx 0.2$ orbits yield a radius $r \simeq 54$ km, while $e \approx 0.05$ orbits yield $r \simeq 58$ km. Note that the effect of the assumed density goes like $\rho^{-1/3}$, so a change of density by a factor of two results in only a 26% variation of the estimated radius. The radius uncertainty thus is dominated by the unknown density rather than one’s conclusion about the mutual semimajor axis and orbital period.

It is reassuring that using two different kinds of measurements (astrometry and photometry) and common assumptions ($\rho \simeq 1 \text{ g cm}^{-3}$ and $p \simeq 0.16$) we get similar results for the inferred size of each component of 2001 QW₃₂₂.

Combining the mass derived from Kepler’s third law and the photometrically derived nominal size $r=54$ km for each component, we compute the density of 2001 QW₃₂₂. For the nominal albedo, the density is in the range 0.8-1.2 g cm^{-3} , which is at the limit between a mostly water-ice body and a mixture of water-ice and rocks. This density is smaller than that measured for the largest KBOs: Pluto and Charon (2.03 ± 0.06 and $1.65 \pm 0.06 \text{ g cm}^{-3}$ respectively; *S19*), Eris ($2.26 \pm 0.25 \text{ g cm}^{-3}$; *S20*) and (136108) 2003 EL₆₁ ($3.0 \pm 0.4 \text{ g cm}^{-3}$; *S21*), but it is

denser than other KBO binaries for which a density have been published: 0.3-0.8 g cm⁻³ for (47171) 1999 TC₃₆ (S22) and 0.5-1.0 g cm⁻³ for (26308) 1998 SM₁₆₅ (S23).

Estimating the hydrostatic pressure at the center of each component by

$$P_0 = \frac{2}{3}\pi G\rho^2 r^2 \quad (S6)$$

(e.g. Stansberry *et al.*, 2006), we find $P_0 \simeq 0.4$ MPa. This pressure is insufficient to remove much void space out of cold, particulate water-ice (S24), allowing a rather large porosity of both components and potentially a sizeable fraction of rocky material to be incorporated in them.

Formation scenarios and constraints from the orbit

All formation scenarios proposed to date involve three or more bodies. Formation scenarios by collision (reaccretion of the fragments of a crater or of the fully disrupted body, or rotational fission induced by an impact), involving only two precursor bodies, tend to create smaller secondary-to-primary mass ratios and smaller separation binaries. Rotational fission (involving only one body) followed by tidal evolution produce binaries with angular momentum one order of magnitude smaller than the KBO binaries with wide separations between components (S25, S26). This angular momentum deficit is also the rule for direct-collision formation scenarios (S25, S27-S31).

Four main scenarios have been proposed to explain the formation of Kuiper Belt binaries (S32-S35), each with their own characteristic outcomes. Only the collision of two bodies in the Hill sphere of a third one (cL²L, S32) claims to be able to directly form very larger separation binaries. (S33) claim that their mechanism of interaction of two large bodies with a swarm of small planetesimals (L²1) always dominate over cL²L. This is true for the overall efficiency of binary formation, as L²1 is very efficient at small separations. But it is unable to directly generate any binary with such a large separation. Similarly, mechanisms proposed by (S34) and (S35) fall short of producing binaries like 2001 QW₃₂₂.

The exchange reaction proposed by (S34) can produce very large separations, but only with very large mutual-orbit eccentricities. Creating 2001 QW₃₂₂ by this mechanism would require further evolution of the original, large eccentricity binary. Tidal dissipation is usually a good candidate to circularize orbits, although this would reduce the separation in the same process. The circularization timescale (S36), in the most favorable case of synchronous rotation, is given by

$$\tau_e = -\frac{e}{\dot{e}} \simeq \frac{2ae^2}{\dot{a}} = \frac{2Q_s}{21k_{2s}} \left(\frac{m_s}{m_p}\right) \left(\frac{a}{r_s}\right)^5 \frac{1}{n_s}, \quad (S7)$$

where m_s and m_p are the masses of the secondary and primary respectively, r_s is the radius of the secondary, $n_s = 2\pi/P$ is the mutual orbit frequency, Q_s is the secondary component dissipation factor, and k_{2s} its Love number. Values of $Q_s \sim 100$ are usually assumed for small icy bodies, reaching 10 for the most dissipative bodies (S37). k_{2s} values range from 0.1 for

dissipative bodies to 0.0001 for very elastic bodies (S37). For $Q_s/k_{2s} \sim 100$ (a lower limit) $\tau_e \sim 10^{18}$ yr, although (S6) is derived in the favourable case of the components being already despun to synchronous rotation, even that is unlikely. We compute a despinning time scale (S37) of $\gtrsim 2 \times 10^{16}$ yr, so tides clearly have had no appreciable effect on this system.

(S38) studied the long term stability of moderate to large separation Kuiper Belt binaries and concluded that the most efficient mechanism to disrupt them is the direct collision of an interloper onto the secondary and kicking it out of its orbit. Using the same method for the newly determined orbital parameters of 2001 QW₃₂₂, and still assuming our nominal albedo, we estimate a disruption lifetime for 2001 QW₃₂₂ of 0.3-1 Gy. If the formation of 2001 QW₃₂₂ is primordial, likely due to the cL²L mechanism, then it is one of a few survivors of a population at least 100 times larger. 2001 QW₃₂₂ could also be a transitory object, evolving due to perturbation by a swarm of small KBO interlopers. Moderate separation KB binaries (separation of 1-2'') can have their separation gradually changed by small perturbations, either tightening them, or unbinding them over the age of the Solar System. However, asserting the likelihood of this hypothesis would require a better knowledge of the parent population of moderate separation KB binaries.

Fig. S1. Magnitude of Northern component minus magnitude of Southern component for all observations in R -band (VLT R_{BESS} , VLT $R_{SPECIAL}$ and Gemini r filters). Errorbars are $1-\sigma$ uncertainties. The dotted line correspond to the weighted average of all those measurements.

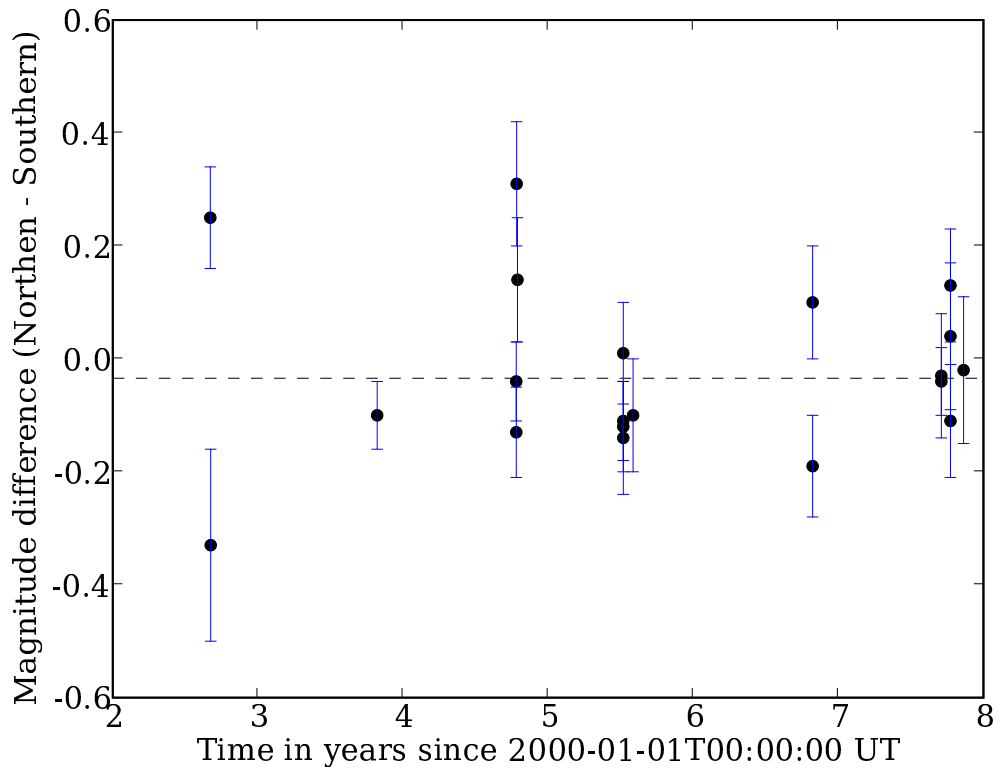


Fig. S2. $g' - r'$ color versus $r' - i'$ color for the Gulbis *et al.* (2006) Kuiper belt core objects (solid circles) and for the two components of 2001 QW₃₂₂ (diamonds). Both components have an $r' - i'$ color that is in the middle of the range for the Core Kuiper belt objects, but a $g' - r'$ color on the blue extreme of it.

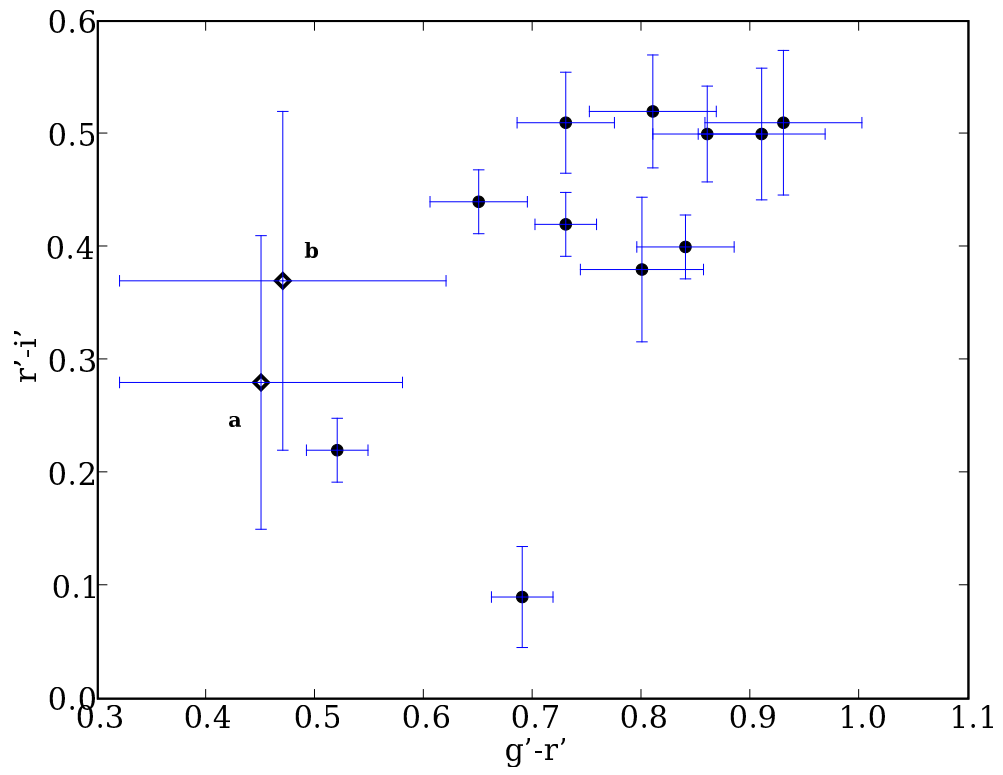


Table S1. List of photometric measurements acquired by our team on 2001 QW₃₂₂ in R band filters (VLT R_{BESS} , VLT $R_{SPECIAL}$ and Gemini r). The second column ($m_b - m_a$) gives the magnitude difference between the 2 components (Northern component minus Southern component) as directly measured from the images, before applying any zeropoint calibration; the uncertainty reported corresponds to the statistical error in the measured flux. The uncertainty is the $1-\sigma$ photon count statistical fluctuation, as reported by the PHOT or ALLSTAR tasks in IRAF. The magnitude reported separately for each component are either absolute photometry directly tied to the Landolt photometric system, or relative to the first measurement in a series (see notes).

UT Date	$m_b - m_a$	m_a	m_b	Filter	Telescope
2002 09 03.00102	0.25 ± 0.09	23.80 ± 0.05	24.04 ± 0.07	R_{BESS}	VLT 8m ^a
2002 09 03.99922	-0.33 ± 0.17	24.18 ± 0.14	23.85 ± 0.11	R_{BESS}	VLT 8m ^a
2003 10 28.01013	-0.10 ± 0.06	23.85 ± 0.05	23.75 ± 0.04	$R_{SPECIAL}$	VLT 8m
2004 10 11.99947	-0.04 ± 0.07	23.81 ± 0.06	23.76 ± 0.06	$R_{SPECIAL}$	VLT 8m ^b
2004 10 12.14095	-0.13 ± 0.08	24.06 ± 0.08	23.86 ± 0.07	$R_{SPECIAL}$	VLT 8m ^b
2004 10 13.13509	0.31 ± 0.11	23.61 ± 0.08	24.01 ± 0.11	$R_{SPECIAL}$	VLT 8m ^b
2004 10 15.16448	0.14 ± 0.11	23.90 ± 0.10	24.05 ± 0.12	$R_{SPECIAL}$	VLT 8m ^b
2005 07 08.44718	-0.11 ± 0.07	23.66 ± 0.05	23.55 ± 0.04	r_{G0303}	Gemini-N 8m
2005 07 08.45190	0.01 ± 0.09	23.72 ± 0.06	23.73 ± 0.06	r_{G0303}	Gemini-N 8m
2005 07 08.49226	-0.12 ± 0.08	23.75 ± 0.06	23.63 ± 0.06	r_{G0303}	Gemini-N 8m
2005 07 08.49698	-0.13 ± 0.10	23.82 ± 0.07	23.69 ± 0.06	r_{G0303}	Gemini-N 8m
2005 08 02.12595	-0.10 ± 0.10	23.92 ± 0.07	23.82 ± 0.07	$R_{SPECIAL}$	VLT 8m
2006 10 28.04920	0.10 ± 0.10			r	Gemini-S 8m
2006 10 28.05355	-0.19 ± 0.09			r	Gemini-S 8m
2007 09 17.01976	-0.03 ± 0.11			r	Gemini-S 8m
2007 09 17.02459	-0.04 ± 0.06			r	Gemini-S 8m
2007 10 10.00426	0.04 ± 0.13	23.96 ± 0.10	24.00 ± 0.10	$R_{SPECIAL}$	VLT 8m ^c
2007 10 10.02030	-0.11 ± 0.10	23.81 ± 0.08	23.70 ± 0.07	$R_{SPECIAL}$	VLT 8m ^c
2007 10 10.03712	0.13 ± 0.10	23.92 ± 0.07	24.05 ± 0.08	$R_{SPECIAL}$	VLT 8m ^c
2007 11 12.03120	-0.02 ± 0.13	23.81 ± 0.09	23.79 ± 0.09	$R_{SPECIAL}$	VLT 8m ^c

^aPhotometry on 2002 09 03.00102 is absolute, tied to the Landolt photometric standard system; other measurements are relative to this one.

^bSame as (^a), but with reference photometry on 2004 10 11.99947.

^cSame as (^a), but with reference photometry on 2007 10 10.00426.

Table S2. Same as Table S1 but for images acquired in V band filters (VLT V_{BESS} and Gemini g).

UT Date	$m_b - m_a$	m_a	m_b	Filter	Telescope
2003 10 28.00556	-0.13 ± 0.09	24.44 ± 0.06	24.31 ± 0.06	V_{BESS}	VLT 8m
2005 07 08.45680	0.03 ± 0.17	24.21 ± 0.11	24.24 ± 0.13	g_{G0301}	Gemini-N 8m
2005 07 08.46152	0.27 ± 0.15	23.94 ± 0.10	24.21 ± 0.12	g_{G0301}	Gemini-N 8m
2005 07 08.48264	-0.29 ± 0.16	24.33 ± 0.13	24.04 ± 0.10	g_{G0301}	Gemini-N 8m
2005 07 08.48737	-0.33 ± 0.17	24.16 ± 0.14	23.83 ± 0.11	g_{G0301}	Gemini-N 8m
2007 10 10.01232	0.00 ± 0.08	24.27 ± 0.06	24.27 ± 0.07	V_{BESS}	VLT 8m

Table S3. Same as Table S1 but for images acquired in I band filters (VLT I_{BESS} and Gemini i).

UT Date	$m_b - m_a$	m_a	m_b	Filter	Telescope
2003 10 28.01355	-0.05 ± 0.09	23.30 ± 0.07	23.25 ± 0.06	I_{BESS}	VLT 8m
2005 07 08.46604	-0.33 ± 0.13	23.63 ± 0.10	23.30 ± 0.08	i_{G0302}	Gemini-N 8m
2005 07 08.47006	-0.30 ± 0.10	23.49 ± 0.07	23.19 ± 0.06	i_{G0302}	Gemini-N 8m
2005 07 08.47409	-0.14 ± 0.09	23.42 ± 0.07	23.28 ± 0.06	i_{G0302}	Gemini-N 8m
2005 07 08.47812	-0.09 ± 0.09	23.40 ± 0.07	23.31 ± 0.06	i_{G0302}	Gemini-N 8m
2007 10 10.02872	0.07 ± 0.07	23.30 ± 0.05	23.37 ± 0.05	I_{BESS}	VLT 8m

Table S4. Separation (in arcseconds) and position angle (PA; origin is North, positive values to the East) for all astrometric observations of 2001 QW₃₂₂. The “UT Date” column corresponds to the time at center of observation, with no light travel time correction applied. The position (RA and DEC columns) is given for the center of mass of the binary, assuming equal masses for the components. The “ δ Sep” column give the uncertainty estimate on the separation (in arcsecond). The uncertainty on the position angle (not given here) is simply δ Sep divided by Sep, in radian. The last column indicates the telescope used to acquire these data.

UT Date	RA	DEC	Sep (")	P.A. (°)	δ Sep (")	Telescope
2001 07 27.42296	20 34 48.37	-18 49 50.4	3.61	-70.0	0.20	CFHT 3.6m ^a
2001 08 24.24085	20 32 43.41	-18 57 51.4	3.89	-68.7	0.17	CFHT 3.6m
2001 08 24.26181	20 32 43.33	-18 57 51.7	3.87	-72.9	0.18	CFHT 3.6m
2001 08 24.28289	20 32 43.24	-18 57 52.0	3.96	-69.9	0.12	CFHT 3.6m
2001 08 25.25689	20 32 39.25	-18 58 07.3	3.74	-67.8	0.23	CFHT 3.6m
2001 08 25.27753	20 32 39.16	-18 58 07.7	3.83	-71.4	0.09	CFHT 3.6m
2001 09 18.16406	20 31 17.28	-19 03 23.0	4.09	-72.0	0.35	Hale 5m ^b
2001 09 18.17234	20 31 17.26	-19 03 23.1	4.23	-67.5	0.35	Hale 5m
2001 09 18.17648	20 31 17.25	-19 03 23.1	3.95	-67.1	0.35	Hale 5m
2001 09 19.18914	20 31 14.60	-19 03 33.5	4.16	-73.2	0.25	Hale 5m
2001 09 19.26248	20 31 14.40	-19 03 34.2	4.38	-79.3	0.53	Hale 5m
2002 06 07.52857	20 43 12.03	-18 23 55.4	3.62	-65.7	0.12	CFHT 3.6m
2002 06 07.53979	20 43 12.00	-18 23 55.5	3.54	-65.0	0.12	CFHT 3.6m
2002 09 03.00102	20 37 16.13	-18 47 51.8	3.47	-65.0	0.05	VLT 8m ^c
2002 09 03.99922	20 37 12.44	-18 48 06.3	3.27	-63.2	0.24	VLT 8m
2003 07 29.05982	20 45 02.95	-18 24 18.4	3.26	-60.2	0.33	ESO 2.2m ^c
2003 07 31.29834	20 44 52.60	-18 25 00.9	3.21	-57.3	0.10	ESO 2.2m
2003 10 28.00556	20 40 46.07	-18 41 47.5	2.93	-55.4	0.06	VLT 8m
2003 10 28.01013	20 40 46.08	-18 41 47.5	2.92	-55.2	0.04	VLT 8m
2003 10 28.01355	20 40 46.08	-18 41 47.5	2.93	-54.9	0.06	VLT 8m
2004 09 16.13690	20 46 45.72	-18 24 48.1	2.62	-43.9	0.35	Hale 5m
2004 09 16.16437	20 46 45.64	-18 24 48.5	2.55	-48.2	0.35	Hale 5m
2004 10 11.99947	20 45 52.88	-18 28 26.4	2.35	-40.9	0.04	VLT 8m
2004 10 12.14095	20 45 52.74	-18 28 27.0	2.37	-42.0	0.04	VLT 8m
2004 10 13.13509	20 45 51.84	-18 28 31.0	2.22	-43.0	0.10	VLT 8m
2004 10 15.16448	20 45 50.27	-18 28 37.9	2.30	-42.2	0.11	VLT 8m
2005 07 08.44718	20 56 46.34	-17 49 58.1	2.00	-25.6	0.04	Gemini-N 8m ^d
2005 07 08.47006	20 56 46.25	-17 49 58.6	2.06	-27.6	0.07	Gemini-N 8m
2005 08 02.12595	20 54 57.80	-17 57 53.8	1.92	-27.9	0.10	VLT 8m
2005 09 26.17135	20 51 24.96	-18 12 53.2	2.00	-24.0	0.12	WIYN 3.5m ^e
2005 09 26.23657	20 51 24.79	-18 12 53.9	1.96	-27.5	0.12	WIYN 3.5m
2005 10 04.11739	20 51 08.31	-18 14 02.6	1.89	-23.1	0.15	Hale 5m

Continued on Next Page ...

Table S4 – Continued

2005 10 04.15318	20 51 08.25	-18 14 02.9	1.87	-27.7	0.14	Hale 5m
2006 10 21.89960	20 55 52.77	-18 01 16.1	1.60	4.1	0.24	WHT 4.2m ^f
2006 10 28.04920	20 55 52.45	-18 01 17.9	1.64	9.1	0.06	Gemini-S 8m ^d
2006 10 28.05355	20 55 52.46	-18 01 17.9	1.66	5.5	0.05	Gemini-S 8m
2007 09 16.19381	21 02 04.68	-17 41 44.0	1.84	32.4	0.18	Hale 5m
2007 09 16.20003	21 02 04.66	-17 41 44.0	1.86	26.7	0.15	Hale 5m
2007 09 16.23572	21 02 04.54	-17 41 44.6	1.83	32.8	0.14	Hale 5m
2007 09 17.01976	21 02 01.99	-17 41 55.5	1.79	32.8	0.07	Gemini-S 8m
2007 09 17.02459	21 02 01.98	-17 41 55.6	1.88	32.5	0.04	Gemini-S 8m
2007 10 10.01232	21 01 06.39	-17 45 53.6	1.80	37.1	0.07	VLT 8m
2007 10 10.02030	21 01 06.38	-17 45 53.6	1.82	34.2	0.05	VLT 8m
2007 10 10.03712	21 01 06.35	-17 45 53.8	1.80	34.2	0.05	VLT 8m
2007 11 03.08849	21 00 55.56	-17 46 38.0	1.83	35.4	0.09	MMT 6.5m ^g
2007 11 03.09269	21 00 55.56	-17 46 38.0	1.92	40.4	0.11	MMT 6.5m
2007 11 12.03120	21 01 05.14	-17 45 57.0	1.85	37.6	0.09	VLT 8m

References and Notes

- S1 J.J. Kavelaars, M.J. Holman, T. Grav, D. Milisavljevic, W. Fraser, B.J. Gladman, J.-M. Petit, P. Rousselot, O. Mousis, P.D. Nicholson, *Icarus*, **169**, 474 (2004).
- S2 J.J. Kavelaars, J.-M. Petit, G. Gladman, M. Holman, *IAU Circ.*, **7749**, 1 (2001).
- S3 J.L. Margot, M.C. Nolan, V. Negron, A.A. Hine, D.B. Campbell, E.S. Howell, L.A.M. Benner, S.J. Ostro, J.D. Giorgini, B.G. Marsden, *IAU Circ.*, **8227**, 1 (2003).
- S4 R. Behrend and 48 colleagues, *Astron. Astrophys.*, **446**, 1177 (2006).
- S5 W.J. Merline, L.M. Close, N. Siegler, D. Potter, C.R. Chapman, C. Dumas, F. Menard, D.C. Slater, A.C. Baker, M.G. Edmunds, G. Mathlin, O. Guyon, K. Roth, *IAU Circ.*, **7741**, 1 (2001).
- S6 K.S. Noll, W.M. Grundy, E.I. Chiang, J.L. Margot, S.D. Kern, in *The Solar System beyond Neptune*, A. Barucci, H. Boehnhardt, D. Cruikshank, A. Morbidelli Eds. (Univ. Arizona Press, Tucson, AZ, 2008), pp. 345-363.
- S7 B. Gladman, B.G. Marsden, C. Van Laerhoven, in *The Solar System beyond Neptune*, A. Barucci, H. Boehnhardt, D. Cruikshank, A. Morbidelli Eds. (Univ. Arizona Press, Tucson, AZ, 2008), pp. 43-57.
- S8 H.H. Russell, *Astrophys. J.*, **43**, 173 (1916).
- S9 <http://www.ucolick.org/~cnaw/sun.html>
- S10 G. Bruzual, S. Charlot, *MNRAS*, **344**, 1000 (2003).
- S11 M. Fukugita, K. Shimasaku, T. Ichikawa, *PASP*, **107**, 945 (1995).
- S12 J.L. Margot, M.E. Brown, C.A. Trujillo, R. Sari, J.A. Stansberry, *Bull. Amer. Astron. Soc.*, **37**, 737 (2005).
- S13 O.R. Hainaut, A.C. Delsanti, *Astron. Astrophys.*, **389**, 641 (2002).
- S14 A.A.S. Gulbis, J.L. Elliot, J.F. Kane, *Icarus*, **183**, 168 (2006).
- S15 J.L. Margot, M.C. Nolan, L.A.M. Benner, S.J. Ostro, R.F. Jurgens, J.D. Giorgini, M.A. Slade, D.B. Campbell, *Science*, **296**, 1445 (2002).
- S16 S.J. Ostro, J.L. Margot, L.A.M. Benner, J.D. Giorgini, D.J. Scheeres, E.G. Fahnestock, S.B. Broschart, J. Bellerose, M.C. Nolan, C. Magri, P. Pravec, P. Schleirich, R. Rose, R.F. Jurgens, E.M. De Jong, S. Suzuki, *Science*, **314**, 1276 (2006).
- S17 J.L. Margot, M.E. Brown, *Science*, **300**, 1939 (2003).

- S18 W.J. Merline, S.J. Weidenschilling, D.D. Durda, J.L. Margot, P. Pravec and A.D. Storrs, in *Asteroids III*, W.F. Bottke Jr., A. Cellino, P. Paolicchi, R.P. Binzel Eds. (Univ. Arizona Press, Tucson, AZ, 2002), pp. 289-312.
- S19 M.W. Buie, W.M. Grundy, E.F. Young, L.Y. Young, S.A. Stern, *Astron. J.*, **132**, 290 (2006).
- S20 M.E. Brown, *Invited talk at AAS/DPS meeting, Pasadena, CA, 2006 October 9-13*.
- S21 D.L. Rabinowitz, K. Barkume, M.E. Brown, H. Roe, M. Schwartz, S. Tourtellotte, C. Trujillo, *Astrophys. J.*, **639**, 1238 (2006).
- S22 J.A. Stansberry, W.M. Grundy, J.L. Margot, D.P. Cruikshank, J.P. Emery, G.H. Rieke, D.T. Trilling, *Astrophys. J.*, **643**, 556 (2006).
- S23 J.R. Spencer, J.A. Stansberry, W.M. Grundy, K.S. Noll, *Bull. Am. Astron. Soc.*, **38**, 546 (2006).
- S24 W.B. Durham, W.B. McKinnon, L.A. Stern, *Geophys. Rev. Lett.*, **32**, L18202.1 (2005).
- S25 J.L. Margot, *Nature*, **416**, 694 (2002).
- S26 S.J. Weidenschilling, *Icarus*, **46**, 124 (2001).
- S27 J.A. Burns, *Nature*, **427**, 494 (2004).
- S28 D.D. Durda, W.F. Bottke, B.L. Enke, W.J. Merline, E. Asphaug, D.C. Richardson, Z.M. Leinhardt, *Icarus*, **167**, 382 (2004).
- S29 S.A. Stern, *Astron. J.*, **124**, 2300 (2002).
- S30 R.M. Canup, *Science*, **307**, 546 (2005).
- S31 E. Chiang, Y. Lithwick, R. Murray-Clay, M. Buie, W.M. Grundy, M. Holman, in *Protostars and Planets V*, B. Reipurth, D. Jewitt, K. Keil Eds. (Univ. Arizona Press, Tucson, AZ, 2006), pp. 895-911.
- S32 S.J. Weidenschilling, *Icarus*, **160**, 212 (2002).
- S33 P. Goldreich, Y. Lithwick, R. Sari, *Nature*, **420**, 643 (2002).
- S34 Y. Funato, J. Makino, P. Hut, E. Kokubo, D. Kinoshita, *Nature*, **427**, 518 (2004).
- S35 S.A. Astakhov, E.A. Lee, D. Farrelly, *MNRAS*, **360**, 401 (2005).
- S36 C.F. Chyba, D.G. Jankowski, P.D. Nicholson, *Astron. Astrophys.*, **219**, L23 (1989).

S37 C.D. Murray, S.F. Dermott, *Solar System Dynamics* (Cambridge University Press, 2000), p. 166.

S38 J-M. Petit, O. Mousis, *Icarus*, **168**, 409 (2004).